

Conversion of Methane into Methanol Using the [6,6'-(2,2'-Bipyridine-6,6'-Diyl)bis(1,3,5-Triazine-2,4-Diamine)](Nitrato-O)Copper(II) Complex in a Solid Electrolyte Reactor Fuel Cell Type

Luis M. S. Garcia, Sanil Rajak, Khaoula Chair, Camila M. Godoy, Araceli Jardim Silva, Paulo V. R. Gomes, Edgar Aparecido Sanches, Andrezza S. Ramos, Rodrigo F. B. De Souza, Adam Duong,* and Almir O. Neto*



Cite This: *ACS Omega* 2020, 5, 16003–16009



Read Online

ACCESS |

Metrics & More

Article Recommendations

ABSTRACT: The application of solid electrolyte reactors for methane oxidation to co-generation of power and chemicals could be interesting, mainly with the use of materials that could come from renewable sources and abundant metals, such as the [6,6'-(2,2'-bipyridine-6,6'-diyl)bis(1,3,5-triazine-2,4-diamine)](nitrate-O)copper (II) complex. In this study, we investigated the optimal ratio between this complex and carbon to obtain a stable, conductive, and functional reagent diffusion electrode. The most active Cu-complex compositions were 2.5 and 5% carbon, which were measured with higher values of open circuit and electric current, in addition to the higher methanol production with reaction rates of $1.85 \text{ mol L}^{-1} \text{ h}^{-1}$ close to the short circuit potential and $1.65 \text{ mol L}^{-1} \text{ h}^{-1}$ close to the open circuit potential, respectively. This activity was attributed to the ability of these compositions to activate water due to better distribution of the Cu complex in the carbon matrix as observed in the rotating ring disk electrode experiments.



1. INTRODUCTION

The emission of greenhouse gases is a major air pollution that causes climate change in the world. In addition to carbon dioxide (CO_2), methane (CH_4) is the second most harmful gas that negatively impacts the atmosphere.¹ Methane, when exposed to the atmosphere, undergoes photochemical degradation by the hydroxyl radical (OH), which is the main atmospheric oxidant of most tropospheric pollutants.² Methane is widely used as an energy source, having reserves as large as oil.^{3–5} This gas can also be produced continuously by the anaerobic oxidation of organic material.⁶

Unlike oil, methane gas is used primarily as a fuel.^{7,8} Methane is a small molecule that has the high energy of the C–H bond (435 kJ mol^{-1}) and a tetrahedral shape that makes it difficult to polarize.⁹ Nonetheless, partial methane oxidation products, such as methanol (CH_3OH) and methyl formate (CHOOCH_3), are of great interest to industry.^{3,9} Several investigations have been conducted to identify a method to convert methane to methanol mainly via conventional catalytic processes, plasma technology, photo-catalysts, supercritical water processes, and biological processes.⁸

Recently, efforts have been devoted to development of methods for partial oxidation of methane to oxygenate products in one step under mild conditions.^{9–12} Galvanic and electrolytic processes are being developed for this purpose with some success.^{8,9,13,14} Among the possible electrochemical reactors, solid electrolyte membrane reactor fuel cells (SEMR-

FCs) are of particular interest. With the ability to operate in electrolytic and galvanic modes, SEMR-FCs perform the reaction in a continuous flow, simultaneously allowing the co-generation of electrical energy and chemicals.^{12,15,16} On the other hand, these reactors depend a lot on the use of noble metals as catalysts (Pt, Pd, and Au),^{9,12,17,18} due to the high stability that these metals have in an electrochemical system.

In the search for noble metal substitutes, the discovery of a variety of new catalytic reactions carried out using low-cost transition metal coordination complexes is promising. Copper complexes are a promising alternative to noble metals. Recently, Chan et al.¹⁹ demonstrated that copper complexes are particularly interesting for partial oxidation of methane. The authors applied tricooper complexes to catalyze the oxidation of methane to methanol and obtained good results. Copper is also widely used for thermal conversion of methane to products, as well as to improve catalytic performance at low temperatures.²⁰ In addition, copper in an alkaline medium is a good catalyst for water activation,²¹ a very important reaction for the partial oxidation of methane. This reaction occurs due

Received: March 26, 2020

Accepted: June 1, 2020

Published: June 25, 2020

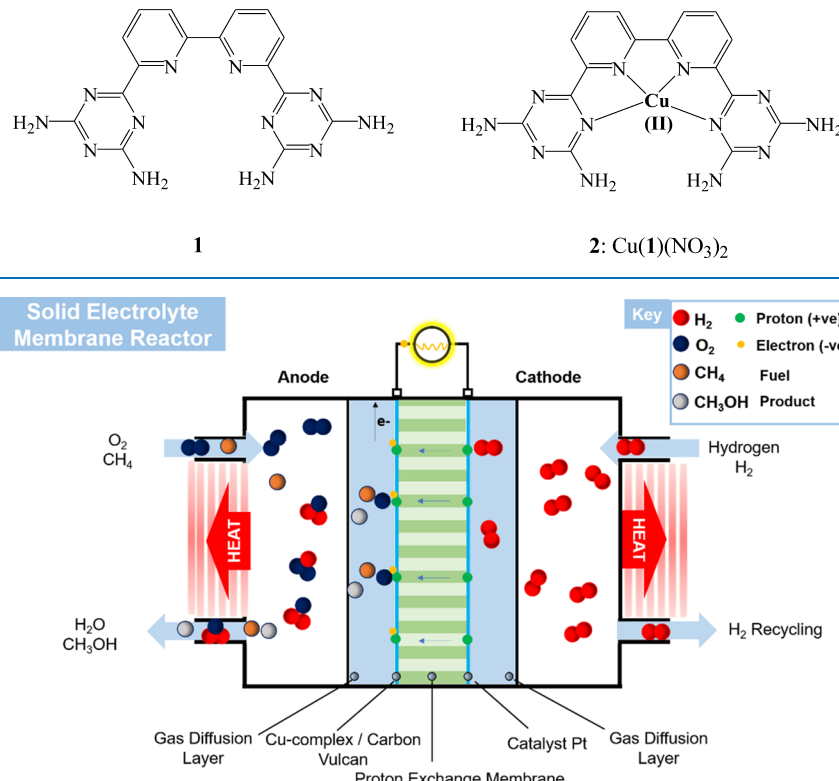


ACS Publications

© 2020 American Chemical Society

16003

<https://dx.doi.org/10.1021/acsomega.0c01363>
ACS Omega 2020, 5, 16003–16009

Scheme 1. Molecular Structure of Ligand 1 and Cu-Complex 2**Figure 1.** Solid electrolyte reactor.

to the generation of hydroxyl radicals that produce methanol and methyl formate from methane.^{22,23} The present work investigates the conversion of methane to methanol using the [6,6'-(2,2'-bipyridine-6,6'-diyl)bis(1,3,5-triazine-2,4-diamine)](nitrate-O)copper(II) complex (Scheme 1) in a SEMR-FC type.

Complex 2 has been chosen because it contains copper (II) and because of its facile synthesis with a high yield. Moreover, this complex is thermally and chemically stable. In addition, 2 is insoluble in water, methane, and methanol, which is adequate to work in heterogeneous conditions. For the catalytic conversion from CH_4 to CH_3OH , our strategy is to use a fuel cell in which the cathode electrode is coated with a mixture of Carbon Vulcan and a percentage of copper complex 2. In the entrance of the cathode chamber, oxygen and methane gases will be loaded. The gases evacuated at the exit of the chamber will be collected and analyzed to determine the percentage of the methanol obtained. Specifically, the presence of methanol and the quantity produced are determined by FT-IR and Raman spectroscopy, respectively. Figure 1 shows the solid electrolyte reactor used for the production of methanol from methane.

2. EXPERIMENTAL METHODS

6,6'-(2,2'-Bipyridine-6,6'-diyl)bis(1,3,5-triazine-2,4-diamine) 1 and the corresponding copper complex 2 were synthesized according to a reported method.^{24,25} The Cu-complex was physically mixed with Carbon Vulcan in the proportions 1, 2.5, 5, 10, and 20% in carbon (mass/mass) to prepare the catalysts that will be placed in the cathode chamber.

Electrochemical measurements were performed using a three-electrode cell, an Ametek PARSTAT 3000A-DXbi-

potentiostat/galvanostat, and a rotating ring disk (RRD) accessory (Pine Instruments). The working electrode is a rotating ring disk electrode (RRDE), which is composed of a gold ring (area = 0.19 cm^2) and a glassy carbon disk (area = 0.25 cm^2) with a collection factor of 0.37. In the conventional electrochemical cell, Ag/AgCl and Pt were used as the reference electrode and the counter electrode (area = 2 cm^2), respectively. To the working electrodes, $15 \mu\text{L}$ aliquots of each sample were added, which consisted of a previously prepared paint composed of a mixture of 8 mg of catalyst + $750 \mu\text{L}$ of H_2O , $250 \mu\text{L}$ of isopropyl alcohol, and $15 \mu\text{L}$ of 5% Nafion D-520. All experiments with different Cu-complex percentage catalysts were performed in KOH 1 mol L^{-1} aqueous solution. The curves were obtained at different speeds ranging from 100, 400, 600, 900, 1600, and 2500 rpm.

To perform the SEMR-FC tests and to obtain the polarization curves, the membrane electrode assembly (MEA) was made with a Nafion 117 membrane treated with KOH; the Pt/C BASF catalyst (20% by weight) with 1 mg cm^{-2} Pt was used as the cathode in gas diffusion electrodes, and catalysts with different Cu-complex ratios served as the anode. The reactor, a cell with ElectroChem unit-type serpentine distribution, was supplied with CH_4 at a flow rate of 50 mL min^{-1} and 1.0 mol L^{-1} KOH at a flow rate of 1 mL min^{-1} at room temperature at the anode and external O_2 with the aid of a temperature-controlled humidifier bottle of 80°C with a flow rate of 200 mL min^{-1} at the cathode.

The Fourier transform infrared spectroscopy (FT-IR) technique was used to determine the different species formed during the electrochemical oxidation of methane in the alkaline medium at different potentials. Anodic reaction products were collected by 300 s increments of 50 mV and analyzed by ATR-

FTIR performed on an ATR accessory (MIRacle with a ZnSe Crystal Plate Pike) installed on a Nicolet 6700 FT-IR spectrometer equipped with a cooled MCT detector with liquid N₂. Raman spectroscopy was used for characterization and quantitative determination of the obtained products. To quantify the methanol concentration obtained from the solutions collected in the solid membrane reactor (SMR), the method applied by Boyaci et al.²⁶ and Santos et al.¹² was used, using Horiba Scientific MacroRam Raman spectroscopy equipment. The wavelength was set at 785 nm.

3. RESULTS AND DISCUSSION

As the catalytic reaction involves electron transfer, we first study the electrochemistry of the catalyst (mixture of Cu-

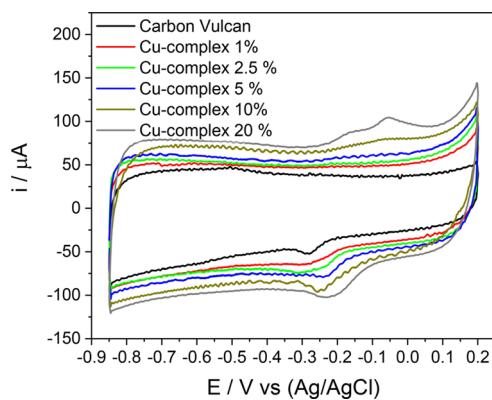


Figure 2. Cyclic voltammetry of Cu-complex/Carbon Vulcan material in 1 mol L⁻¹ KOH ($v = 10$ mV s⁻¹).

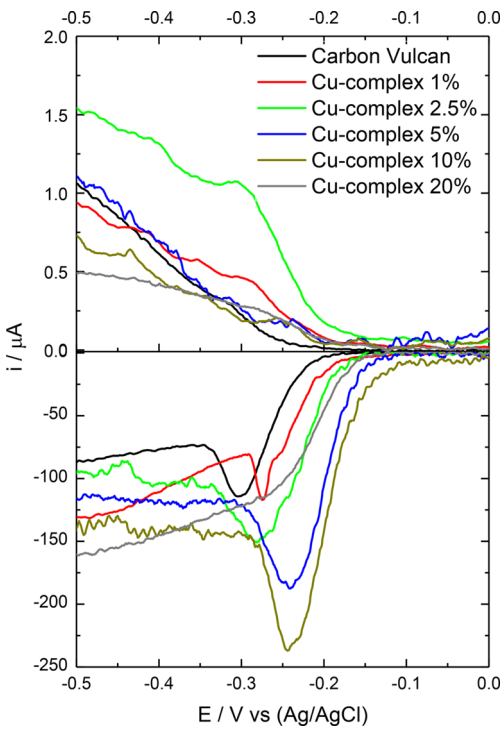


Figure 3. RRDE voltammograms at 1600 r.p.m. in O₂-unsaturated electrolyte with the disk current, ring current, and current corresponding to hydrogen peroxide obtained from the ring current.

complex/Carbon Vulcan) by using cyclic voltammetry (CV). This measurement allows evaluation of the potential required

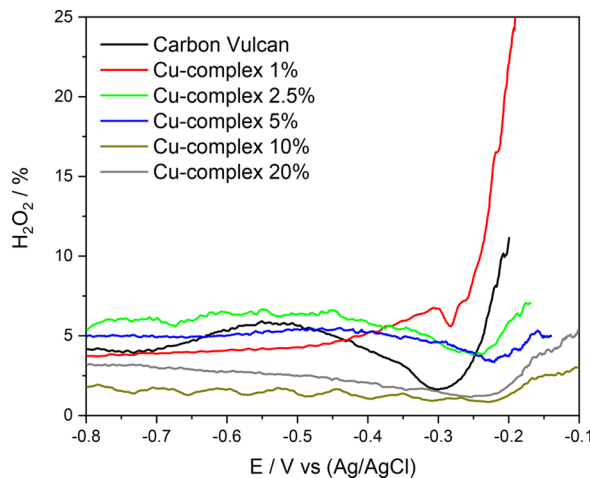


Figure 4. H₂O₂% selectivity as a function of the applied potential.

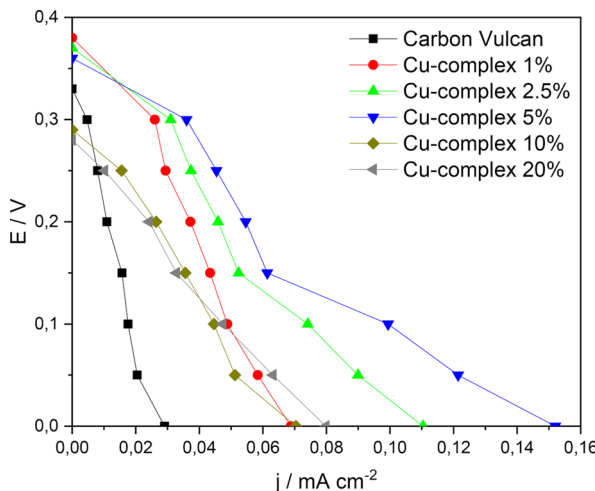
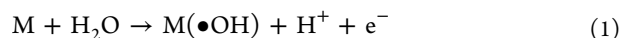


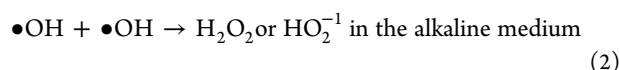
Figure 5. Polarization curves of a 5 cm² SEMR-FC at room temperature using Cu-complex/Carbon Vulcan catalyst anodes (5 mg cm⁻² catalyst loading) and Pt/C BASF as the cathode in all experiments (1 mg cm⁻² Pt catalyst loading with 20 wt % Pt loading on carbon), Nafion 117 membrane treated with KOH 1.0 mol L⁻¹ + CH₄ at 50 mL min⁻¹, and O₂ flux at 200 mL min⁻¹.

to perform the conversion of methane to methanol. Figure 2 shows the CV of the catalyst at several mass ratios of Cu-complex/carbon. As can be seen, an increase in the percentage of the Cu-complex on carbon results in two oxidation peaks at -0.2 and -0.05 V that can be attributed to the formation of copper oxides or surfaces containing copper.^{27,28} The carbon reduction peak at -0.28 V shifts to a slightly higher potential with an increase of intensity and broadness.^{29,30}

For partial oxidation of methane by the electrochemical method, water activation is necessary^{22,23} in which the hydroxyl radicals can be produced directly by the oxidation of water (eq 1).³¹



This radical can be detected indirectly by the formation of hydrogen peroxide generated by the chemical equilibrium of this radical, according to eq 2:³²



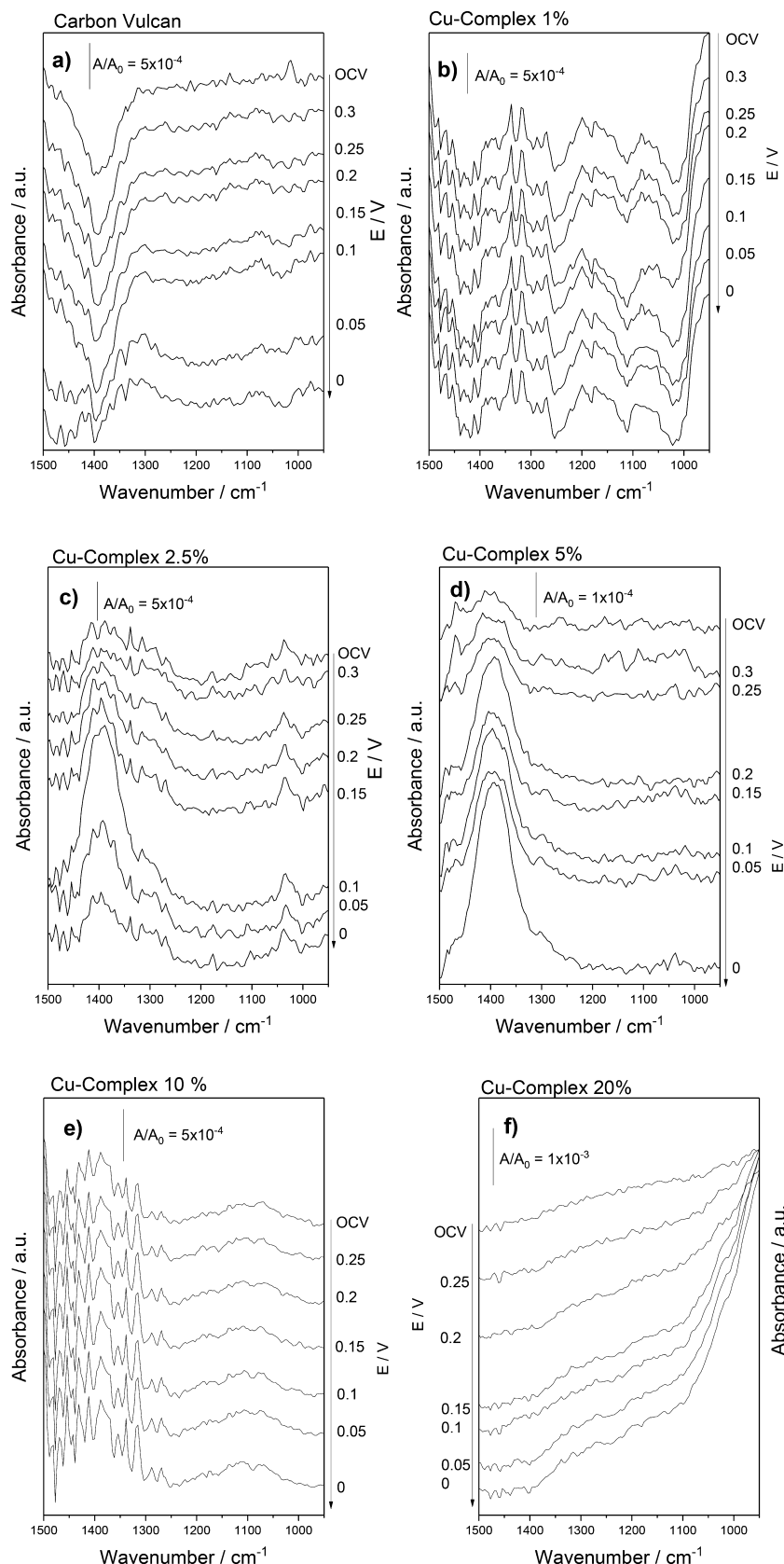


Figure 6. FT-IR spectra of the effluent of the SEMR-FC at several potentials in 1.0 mol L⁻¹ KOH, and the methane flow was set to 50 mL min⁻¹ for (a) Carbon Vulcan, (b) 1% Cu-complex, (c) 2.5% Cu-complex, (d) 5% Cu-complex, (e) 10% Cu-complex, and (f) 20% Cu-complex.

The detection of H₂O₂ electrochemically is carried out by RRDE experiments and thus indicates the most suitable

percentage of the Cu-complex that should be used for the conversion of methane to methanol in the alkaline medium.

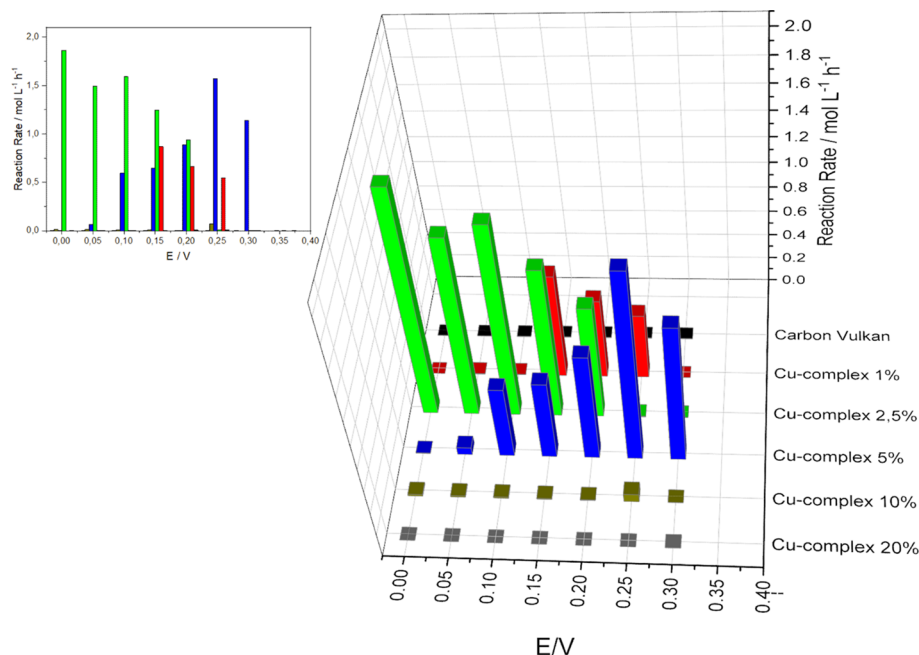


Figure 7. The reaction rate of methanol production in a SEMR-FC as a function of potential.

Figure 3 shows the disk and ring curves for H_2O_2 generation and detection processes. It is noticed that for amounts of **2** incorporated into carbon 1, 2.5, and 5%, a higher quantity of H_2O_2 is detected than for the other percentage of the mixture of Cu-complex/carbon. The ring current also indicates the potential for completion of the peroxide generation process. As can be seen in **Figure 3**, the increase in the percentage of the Cu-complex produced a shift in higher potential as compared with the Carbon Vulcan (Carbon Vulcan = −0.22 V, Cu-complex 1% = −0.19 V, Cu-complex 2.5% = −0.17 V, Cu-complex 5% = −0.14 V, Cu-complex 10% = −0.12 V, and Cu-complex 20% = −0.1 V).

This difference in the ring current and hence in the amount of peroxide detected can be explained by the change in the oxidation state of the Cu-complex, which can affect the amount of oxygen close to the active sites, thereby creating an optimal chemical environment for the activation of water, as reported by Assumpção et al.³³ The selectivity for the formation of peroxide (% H_2O_2) can be calculated using³⁴

$$\text{H}_2\text{O}_2\% = \frac{200I_r/N}{I_d + I_r/N} \quad (3)$$

where I_d is the disk current, I_r is the ring current, and N is the RRDE collection efficiency (0.37). The calculated results are presented in **Figure 4**, where the $\text{H}_2\text{O}_2\%$ lines in the potential range from −0.8 to −0.3 V, and H_2O_2 yields are ~6, ~5, ~4, and 1% when Cu-complex percentage is Cu-Complex 2.5, 5, 1, and 10%–20% respectively. It is thus observed using the disk–ring curves (**Figure 3**) that although the percentage of **2** is 1%, the production of peroxide is proportional to the current obtained for Cu-complex 5%. When we analyzed the H_2O_2 conversion, this composition presents different efficiencies.

Figure 5 presents the polarization curves of the SEMR-FC for different Cu-complex proportions with KOH and methane fed on the anode. The results are in agreement with those obtained from the electrochemical studies: (i) a low Cu-complex percentage (1, 2.5, and 5) presents an open circuit

voltage (OCV) about 20% higher than that of catalysts with Cu-complex 10 and 20%. The value of our OCV is comparable to the one reported in the literature for methane oxidation with low-temperature fuel cells (about 0.3–0.4 V).^{9,12,35,37} Lee et al. presented several ($\text{V}_2\text{O}_5/\text{SnO}_2$, Pd, Au, and Cu) catalysts with OCV values (0 to −0.4 V) for the conversion of methane to methanol at temperatures below 400 °C. Santos et al. presented (Pt/C, Ni/C, and Pd/C) catalysts with OCV values (0.2 to −0.35 V) at room temperature. Nandehna et al. presented (Pd, Pt, and Zn) catalysts with OCV values (0.2 to 0.3 V) at 80 °C.³⁶ From our results, we concluded that the catalysts are more selective for H_2O_2 when **2** percentages are 2.5 and 5%.

Figure 6 shows IR spectra of the SEMR-FC effluent to identify possible partial oxidation products of methane. For Carbon Vulcan, it is observed that with the decreasing potential, the band centered at $\sim 1302\text{ cm}^{-1}$ increases, corresponding to degeneration of methane.^{37,38} In the case of catalysts with 1, 2.5, and 5%, the absorption bands are more definite as compared with those observed with 10 and 20%. This may be explained by the increase of methane solubility in solution, due to an increase in small organic molecules formed from the partial oxidation of the hydrocarbon.¹²

The methanol production over Cu-complex/Carbon Vulcan is evidenced by $\delta(\text{CH}_3)$ bands at 1482, 1080, and 1030 cm^{-1} (**Figure 6d**).^{12,39} For Carbon Vulcan, these signals are present since the OCV corresponds to 0 V with low resolution. In the Cu-complex, these bands appear in a range of OCV until 0.15 V for 1%, 0.25–0 V for 2.5%, OCV–0 V for 5%, and OCV–0 V with low resolution for 10% and do not appear at all for 20%.

The band centered at 1345 cm^{-1} corresponds to $\nu_{(\text{COO})}$ of solution formate,⁴⁰ which is probably due to the methanol oxidation reaction occurring only for Cu-complex 1% at all potentials, indicating that this composition can promote higher oxidation of the methane than others. For Cu-complex 2.5 and 5% also, a band at 1376 cm^{-1} is detected, which corresponds to carbonate ions,^{41,42} products of complete oxidation of the methane.

The reaction rate (r) of methanol production is calculated with eq 4 using the methanol amount quantified by Boyaci's method²⁶ with the analytical curve constructed in the methanol concentration range of 0.005–1.000 mol L⁻¹. For the following analytical curve, an intensity = 5.14676 + 6.35603 [methanol] is obtained with the correlation coefficient being 0.925.

$$r = \frac{\text{methanol amount}}{\text{volume} \times \text{time}} \quad (4)$$

In the sample containing only carbon, the reaction rate of methanol production as a function of the potential is not significant (Figure 7). The same is observed for the Cu-complex 20% (Figure 6). However, for the other compositions, the potential production of methanol from methane is observed at an appreciable rate. The most active composition is 2.5%, which produces rates greater than 1 mol L⁻¹ h⁻¹ and decreases from 0.2 to 0 V where $r = 1.85$ mol L⁻¹ h⁻¹. The 5% composition has an inverse behavior, with the highest r (1.65 mol L⁻¹ h⁻¹) close to the open circuit potential (0.3 V), which decreases with the potential.

The highest conversion rates were obtained for Cu-complex compositions that mostly produced hydrogen peroxide, indicating that water activation is the determining point for the catalyst applied in the SEMR-FC, confirming the evidence already shown by other researchers.^{9,12,22,23,39}

4. CONCLUSIONS

The Cu-complex, when added in adequate amounts to carbon, improves the production of peroxide, functioning as a dopant. When applied as an anodic catalyst in the SEMR-FC, it was effective in converting methane to methanol. It is observed from Figure 4 that, for amounts greater than 10% of 2, the materials are inefficient in activating water and generating hydroxyl radicals, which prevents the conversion of methane into methanol. From the polarization curves, it is possible to observe that the potentials for the highest amounts of the Cu-complex (10 and 20%) are very close to the lowest percentage (1%). According to our results, percentages of 2.5 and 5% of 2 were the ideal quantities for applications in SEMR-FCs to produce methanol from methane.

■ AUTHOR INFORMATION

Corresponding Authors

Adam Duong — Département de Chimie, Biochimie et Physique, Institut de Recherchesur l'Hydrogène, Université du Québec à Trois-Rivières, Trois-Rivières, Québec G9A5H7, Canada;  orcid.org/0000-0002-4927-3603; Email: adam.duong@uqtr.ca

Almir O. Neto — Instituto de PesquisasEnergéticas e Nucleares, 05508-000 São Paulo, SP, Brazil;  orcid.org/0000-0002-9287-6071; Email: aolivei@ipen.br

Authors

Luis M. S. Garcia — Instituto de PesquisasEnergéticas e Nucleares, 05508-000 São Paulo, SP, Brazil; Département de Chimie, Biochimie et Physique, Institut de Recherchesur l'Hydrogène, Université du Québec à Trois-Rivières, Trois-Rivières, Québec G9A5H7, Canada

Samir Rajak — Département de Chimie, Biochimie et Physique, Institut de Recherchesur l'Hydrogène, Université du Québec à Trois-Rivières, Trois-Rivières, Québec G9A5H7, Canada

Khaoula Chair — Département de Chimie, Biochimie et Physique, Institut de Recherchesur l'Hydrogène, Université du Québec à Trois-Rivières, Trois-Rivières, Québec G9A5H7, Canada

Camila M. Godoy — Instituto de PesquisasEnergéticas e Nucleares, 05508-000 São Paulo, SP, Brazil

Araceli Jardim Silva — Instituto de PesquisasEnergéticas e Nucleares, 05508-000 São Paulo, SP, Brazil

Paulo V. R. Gomes — Department of Chemistry, Federal University of Amazonas, Manaus, Amazonas 69067-005, Brazil

Edgar Aparecido Sanches — Department of Chemistry, Federal University of Amazonas, Manaus, Amazonas 69067-005, Brazil

Andrezza S. Ramos — Instituto de PesquisasEnergéticas e Nucleares, 05508-000 São Paulo, SP, Brazil

Rodrigo F. B. De Souza — Instituto de PesquisasEnergéticas e Nucleares, 05508-000 São Paulo, SP, Brazil;  orcid.org/0000-0003-1501-1274

Complete contact information is available at:

<https://pubs.acs.org/10.1021/acsomega.0c01363>

Notes

The authors declare no competing financial interest.

■ ACKNOWLEDGMENTS

We are grateful to CAPES, FAPESP (2014/09087-4, 2014/50279-4, and 2017/11937-4), CNPQ (300816/2016-2), the Natural Sciences and Engineering Research Council of Canada (RGPIN-2015-06425), the Canada Foundation for Innovation, the Canadian Queen Elizabeth II Diamond Jubilee Scholarships, and the Université du Québec à Trois-Rivières for financial support.

■ REFERENCES

- (1) Kinnunen, N. M.; Hirvi, J. T.; Suvanto, M.; Pakkanen, T. A. Role of the Interface between Pd and PdO in Methane Dissociation. *J. Phys. Chem. C* **2011**, *115*, 19197–19202.
- (2) Bousquet, P.; Ciais, P.; Miller, J. B.; Dlugokencky, E. J.; Hauglustaine, D. A.; Prigent, C.; Van der Werf, G. R.; Peylin, P.; Brunke, E. G.; Carouge, C.; Langenfelds, R. L.; Lathière, J.; Papa, F.; Ramonet, M.; Schmidt, M.; Steele, L. P.; Tyler, S. C.; White, J. Contribution of anthropogenic and natural sources to atmospheric methane variability. *Nature* **2006**, *443*, 439–443.
- (3) Han, B.; Yang, Y.; Xu, Y.; Etim, U. J.; Qiao, K.; Xu, B.; Yan, Z. A review of the direct oxidation of methane to methanol. *Chin. J. Catal.* **2016**, *37*, 1206–1215.
- (4) Arndt, S.; Otremba, T.; Simon, U.; Yildiz, M.; Schubert, H.; Schomäcker, R. Mn–Na₂WO₄/SiO₂ as catalyst for the oxidative coupling of methane. What is really known? *Appl. Catal., A* **2012**, *425-426*, 53–61.
- (5) Gambo, Y.; Jalil, A. A.; Triwahyono, S.; Abdulrasheed, A. A. Recent advances and future prospect in catalysts for oxidative coupling of methane to ethylene: A review. *J. Ind. Eng. Chem.* **2018**, *59*, 218–229.
- (6) Jacquinot, P.; Müller, B.; Wehrli, B.; Hauser, P. C. Determination of methane and other small hydrocarbons with a platinum–Nafion electrode by stripping voltammetry. *Anal. Chim. Acta* **2001**, *432*, 1–10.
- (7) Zhang, Y.; Deng, J.; Zhang, L.; Qiu, W.; Dai, H.; He, H. AuOx/Ce_{0.6}Zr_{0.3}Y_{0.1}O₂ nano-sized catalysts active for the oxidation of methane. *Catal. Today* **2008**, *139*, 29–36.
- (8) Zakaria, Z.; Kamarudin, S. K. Direct conversion technologies of methane to methanol: An overview. *Renewable Sustainable Energy Rev.* **2016**, *65*, 250–261.

- (9) Lee, B.; Hibino, T. Efficient and selective formation of methanol from methane in a fuel cell-type reactor. *J. Catal.* **2011**, *279*, 233–240.
- (10) Wang, B.; Albarracín-Suazo, S.; Págán-Torres, Y.; Nikolla, E. Advances in methane conversion processes. *Catal. Today* **2017**, *285*, 147–158.
- (11) Ma, M.; Jin, B. J.; Li, P.; Jung, M. S.; Kim, J. I.; Cho, Y.; Kim, S.; Moon, J. H.; Park, J. H. Ultrahigh Electrocatalytic Conversion of Methane at Room Temperature. *Adv. Sci.* **2017**, *4*, 1700379.
- (12) Santos, M. C. L.; Nunes, L. C.; Silva, L. M. G.; Ramos, A. S.; Fonseca, F. C.; de Souza, R. F. B.; Neto, A. O. Direct Alkaline Anion Exchange Membrane Fuel Cell to Converting Methane into Methanol. *ChemistrySelect* **2019**, *4*, 11430–11434.
- (13) Rocha, R. S.; Reis, R. M.; Lanza, M. R. V.; Bertazzoli, R. Electrosynthesis of methanol from methane: The role of V₂O₅ in the reaction selectivity for methanol of a TiO₂/RuO₂/V₂O₅ gas diffusion electrode. *Electrochim. Acta* **2013**, *87*, 606–610.
- (14) Dhiman, S. S.; Shrestha, N.; David, A.; Basotra, N.; Johnson, G. R.; Chadha, B. S.; Gadhamshetty, V.; Sani, R. K. Producing methane, methanol and electricity from organic waste of fermentation reaction using novel microbes. *Bioresour. Technol.* **2018**, *258*, 270–278.
- (15) Sundmacher, K.; Rihko-Struckmann, L. K.; Galvita, V. Solid electrolyte membrane reactors: Status and trends. *Catal. Today* **2005**, *104*, 185–199.
- (16) Pan, Z. F.; Chen, R.; An, L.; Li, Y. S. Alkaline anion exchange membrane fuel cells for cogeneration of electricity and valuable chemicals. *J. Power Sources* **2017**, *365*, 430–445.
- (17) Raj, N. T.; Iniyian, S.; Goic, R. A review of renewable energy based cogeneration technologies. *Renewable Sustainable Energy Rev.* **2011**, *15*, 3640–3648.
- (18) Alcaide, F.; Cabot, P.-L.; Brillas, E. Fuel cells for chemicals and energy cogeneration. *J. Power Sources* **2006**, *153*, 47–60.
- (19) Chan, S. I.; Lu, Y.-J.; Nagababu, P.; Maji, S.; Hung, M.-C.; Lee, M. M.; Hsu, I.-J.; Minh, P. D.; Lai, J. C.-H.; Ng, K. Y.; Ramalingam, S.; Yu, S. S.-F.; Chan, M. K. Efficient Oxidation of Methane to Methanol by Dioxygen Mediated by Tricopper Clusters. *Angew. Chem., Int. Ed.* **2013**, *52*, 3731–3735.
- (20) Kaddeche, D.; Djaidja, A.; Barama, A. Partial oxidation of methane on co-precipitated Ni–Mg/Al catalysts modified with copper or iron. *Int. J. Hydrogen Energy* **2017**, *42*, 15002–15009.
- (21) Farinazzo Bergamo Dias Martins, P.; Papa Lopes, P.; Ticianelli, E. A.; Stamenkovic, V. R.; Markovic, N. M.; Strmcnik, D. Hydrogen evolution reaction on copper: Promoting water dissociation by tuning the surface oxophilicity. *Electrochim. Commun.* **2019**, *100*, 30–33.
- (22) Boyd, M. J.; Latimer, A. A.; Dickens, C. F.; Nielander, A. C.; Hahn, C.; Nørskov, J. K.; Higgins, D. C.; Jaramillo, T. F. Electro-Oxidation of Methane on Platinum under Ambient Conditions. *ACS Catal.* **2019**, *9*, 7578–7587.
- (23) Arnarson, L.; Schmidt, P. S.; Pandey, M.; Bagger, A.; Thygesen, K. S.; Stephens, I. E. L.; Rossmeisl, J. Fundamental limitation of electrocatalytic methane conversion to methanol. *Phys. Chem. Chem. Phys.* **2018**, *20*, 11152–11159.
- (24) Duong, A.; Maris, T.; Lebel, O.; Wuest, J. D. Syntheses and Structures of Isomeric Diaminotriazinyl-Substituted 2,2'-Bipyridines and 1,10-Phenanthrolines. *J. Organic Chem.* **2011**, *76*, 1333–1341.
- (25) Rajak, S.; Schott, O.; Kaur, P.; Maris, T.; Hanan, G. S.; Duong, A. Mimicking 2,2': 6',2":6'',2''-quaterpyridine complexes for the light-driven hydrogen evolution reaction: synthesis, structural, thermal and physicochemical characterizations. *RSC Adv.* **2019**, *9*, 28153–28164.
- (26) Boyaci, I. H.; Genis, H. E.; Guven, B.; Tamer, U.; Alper, N. A novel method for quantification of ethanol and methanol in distilled alcoholic beverages using Raman spectroscopy. *J. Raman Spectrosc.* **2012**, *43*, 1171–1176.
- (27) Ottoni, C. A.; Ramos, C. E. D.; de Souza, R. F. B.; da Silva, S. G.; Spinace, E. V.; Neto, A. O. Glycerol and Ethanol Oxidation in Alkaline Medium Using PtCu/C Electrocatalysts. *Int. J. Electrochem. Sci.* **2018**, *13*, 1893–1904.
- (28) Hosseini, H.; Ahmar, H.; Dehghani, A.; Bagheri, A.; Fakhari, A. R.; Amini, M. M. Au-SH-SiO₂ nanoparticles supported on metal-organic framework (Au-SH-SiO₂@Cu-MOF) as a sensor for electrocatalytic oxidation and determination of hydrazine. *Electrochim. Acta* **2013**, *88*, 301–309.
- (29) Assumpção, M. H. M. T.; De Souza, R. F. B.; Rascio, D. C.; Silva, J. C. M.; Calegaro, M. L.; Gaubeur, I.; Paixão, T. R. L. C.; Hammer, P.; Lanza, M. R. V.; Santos, M. C. A comparative study of the electrogeneration of hydrogen peroxide using Vulcan and Printex carbon supports. *Carbon* **2011**, *49*, 2842–2851.
- (30) Nagaiah, T. C.; Kundu, S.; Bron, M.; Muhler, M.; Schuhmann, W. Nitrogen-doped carbon nanotubes as a cathode catalyst for the oxygen reduction reaction in alkaline medium. *Electrochim. Commun.* **2010**, *12*, 338–341.
- (31) Nidheesh, P. V.; Zhou, M.; Oturan, M. A. An overview on the removal of synthetic dyes from water by electrochemical advanced oxidation processes. *Chemosphere* **2018**, *197*, 210–227.
- (32) Nogami, G.; Nishiyama, Y.; Nakamura, H. New Approach to a Rotating Ring Disk Electrode. *J. Electrochim. Soc.* **1988**, *135*, 877–884.
- (33) Assumpção, M. H. M. T.; De Souza, R. F. B.; Reis, R. M.; Rocha, R. S.; Steter, J. R.; Hammer, P.; Gaubeur, I.; Calegaro, M. L.; Lanza, M. R. V.; Santos, M. C. Low tungsten content of nanostructured material supported on carbon for the degradation of phenol. *Appl. Catal., B* **2013**, *142-143*, 479–486.
- (34) Zhou, R.; Zheng, Y.; Jaroniec, M.; Qiao, S.-Z. Determination of the Electron Transfer Number for the Oxygen Reduction Reaction: From Theory to Experiment. *ACS Catal.* **2016**, *6*, 4720–4728.
- (35) Lee, B.; Sakamoto, Y.; Hirabayashi, D.; Suzuki, K.; Hibino, T. Direct oxidation of methane to methanol over proton conductor/metal mixed catalysts. *J. Catal.* **2010**, *271*, 195–200.
- (36) Nandeha, J.; Nagahama, I.; Yamashita, J.; Fontes, E.; Ayoub, J.; de Souza, R.; Fonseca, F.; Neto, A. Activation of Methane on PdZn/C Electrocatalysts in an Acidic Electrolyte at Low Temperatures. *Int. J. Electrochim. Sci.* **2019**, *14*, 10819–10834.
- (37) Nandeha, J.; Fontes, E. H.; Piasentin, R. M.; Fonseca, F. C.; Neto, A. O. Direct oxidation of methane at low temperature using Pt/C, Pd/C, Pt/C-ATO and Pd/C-ATO electrocatalysts prepared by sodium borohydride reduction process. *J. Fuel Chem. Technol.* **2018**, *46*, 1137–1145.
- (38) Scarano, D.; Bertarione, S.; Spoto, G.; Zecchina, A.; Otero Áreán, C. FTIR spectroscopy of hydrogen, carbon monoxide, and methane adsorbed and co-adsorbed on zinc oxide. *Thin Solid Films* **2001**, *400*, 50–55.
- (39) Nandeha, J.; Piasentin, R. M.; Silva, L. M. G.; Fontes, E. H.; Neto, A. O.; de Souza, R. F. B. Partial oxidation of methane and generation of electricity using a PEMFC. *Ionics* **2019**, *25*, 5077–5082.
- (40) Christensen, P. A.; Linares-Moya, D. The Role of Adsorbed Formate and Oxygen in the Oxidation of Methanol at a Polycrystalline Pt Electrode in 0.1 M KOH: An In Situ Fourier Transform Infrared Study. *J. Phys. Chem. C* **2009**, *114*, 1094–1101.
- (41) Fang, X.; Wang, L.; Shen, P. K.; Cui, G.; Bianchini, C. An in situ Fourier transform infrared spectroelectrochemical study on ethanol electrooxidation on Pd in alkaline solution. *J. Power Sources* **2010**, *195*, 1375–1378.
- (42) Fontes, E. H.; Piasentin, R. M.; Ayoub, J. M. S.; da Silva, J. C. M.; Assumpção, M. H. M. T.; Spinacé, E. V.; Neto, A. O.; de Souza, R. F. B. Electrochemical and in situ ATR-FTIR studies of ethanol electro-oxidation in alkaline medium using PtRh/C electrocatalysts. *Mater. Renewable Sustainable Energy* **2015**, *4*, 3.